

Atomic structure of diamond {111} surfaces etched in oxygen water vapor

F. K. de Theije, M. F. Reedijk, J. Arsic, W. J. P. van Enckevort, and E. Vlieg*

Department of Solid State Chemistry, Faculty of Science, University of Nijmegen, The Netherlands

(Received 3 November 2000; published 1 August 2001)

The atomic structure of the {111} diamond face after oxygen–water-vapor etching is determined using x-ray scattering. We find that a single dangling bond diamond {111} surface model, terminated by a full monolayer of —OH fits our data best. To explain the measurements it is necessary to add an ordered water layer on top of the —OH terminated surface. The vertical contraction of the surface cell and the distance between the oxygen atoms are generally in agreement with model calculations and results on similar systems. The OH termination is likely to be present during etching as well. This model experimentally confirms the atomic-scale mechanism we proposed previously for this etching system.

DOI: 10.1103/PhysRevB.64.085403

PACS number(s): 81.65.Cf, 61.10.—i, 68.08.Bc

I. INTRODUCTION

It is well known that growth of chemical-vapor-deposited (CVD) diamond is a complicated process of simultaneous growth and etching, although the exact mechanisms are unclear. One of the compounds that has an important influence on this process is oxygen.^{1–3} Addition of small amounts of oxygen enhances the growth rate and improves the crystalline quality of the grown layers.⁴ Therefore, the interaction of oxygen with diamond surfaces is studied quite intensively, both by theoreticians and by experimentalists. Oxygen in the gas phase is able to remove non-diamond-bonded carbon from the surface. This etching occurs probably via OH, which is formed in the gas phase upon addition of O₂,⁵ and is much more effective than H alone.⁶

Most theoretical studies on the interaction of oxygen with diamond have been concerned with the chemisorption of oxygen on diamond {001} surfaces.^{7–12} The stable configurations for diamond {001} in the presence of both oxygen and hydrogen were studied by Skokov, Weiner, and Frenklach.¹³ They found that surfaces containing —OH and O-bridge groups are energetically more favorable than surfaces containing oxygen on top. This is because hydrogen bonds can be formed among the chemisorbed species. Diamond {111} faces are studied less extensively. On oxidized {111} faces C-O-C, C-O-O-C, and C-O structures are calculated, with a strong similarity in energy. Therefore, these systems may coexist.¹² To our knowledge, the interactions of diamond {111} with both oxygen and hydrogen have not been calculated. It is clear that because of the different geometry of {001} and {111} diamond faces, the surface interactions with either oxygen or OH-containing groups will differ for these two faces.

The experimental research on the surface chemistry of diamond oxidation is also mostly performed on {001} diamond surfaces and on diamond powder. A summary of the present status in this field is given in Ref. 14. Very recently, two papers on this subject were published by Pehrsson and Mercer.^{15,16} They oxidized hydrogenated diamond {001} by leaking thermally activated oxygen in their ultrahigh vacuum (UHV) system. Below 80 °C, a full monolayer coverage was obtained and C=O, C-O-C, and —OH groups were observed. At higher temperatures, the oxygen desorption was

much faster and the peak coverage was much lower.

Klauser *et al.*¹⁷ studied the adsorption of O and H on {111} diamond under high-vacuum conditions at room temperature. Their measurements show the bonding of oxygen atoms to the C{111}-(2×1) π -bonded chains. H atoms exposed to the O/C {111} surface replace the O atoms and convert the surface to (1×1):H, while atomic O cannot do the same to preadsorbed H. Surface x-ray measurements on polished {111}-(1×1) diamond in UHV shows that the surface is mostly H-terminated, but contains also O, most likely in the form of —OH, and C in the form of —CH₃.¹⁸ Most experimental studies were done under UHV conditions, whereas our etching experiments are done at atmospheric pressure. A recent paper by Steadman *et al.*¹⁹ showed that the interaction of species with a surface may depend strongly on the pressure.

In earlier experiments^{14,20,21} we studied the mechanisms for various oxidative etching methods of diamond by investigating the morphology and etch rates. Of these methods, etching in oxygen/water provides the most relevant information on the processes during CVD diamond growth, because during CVD the gas phase typically contains hydrocarbons and hydrogen. Therefore, CVD environments containing oxygen are in most cases also rich in hydrogen atoms. For diamond {111} etched in oxygen/water we proposed a structure where the single dangling bond at the surface is stabilized by monovalent compounds, e.g., —OH and —H. Here we present a surface x-ray diffraction study of the {111} surface after etching in O₂ and water. In agreement with our previous conjecture, we find that the surface is —OH terminated.

II. EXPERIMENT

The measurements are performed on cleaved {111} diamond surfaces with a miscut <1°. Both a synthetic and a natural diamond crystal are used, with a size of 3×3×1 and 4×3×0.5 mm³, respectively. Atomic force microscopic (AFM) measurements show flat terraces, 50–1000-nm wide (see Fig. 1). These terraces are large enough to allow x-ray diffraction experiments. The terraces on the natural diamond are generally somewhat larger compared to those on the synthetic diamond. This is also reflected in the x-ray measure-

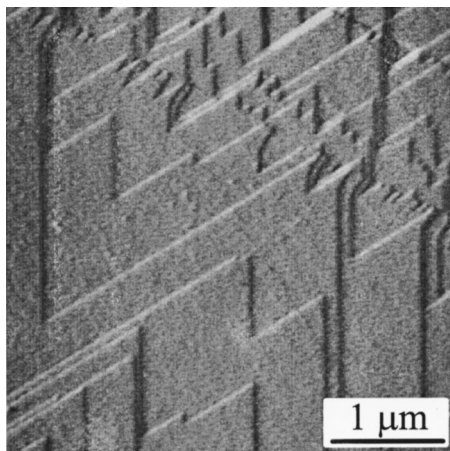


FIG. 1. AFM image of the natural diamond $\{111\}$ surface before etching. The large flat terraces indicate that this surface is suitable for x-ray diffraction experiments.

ments, which yield better results on the natural diamond. The step height is $2.0 \pm 0.3 \text{ \AA}$, corresponding to one atomic layer.

A. Diamond etching experiments

In order to determine the complexes that account for the etching of diamond $\{111\}$ in oxygen/water, the cleaved diamond $\{111\}$ surfaces are etched *in situ*. For this, we have constructed a temperature-stabilized sample chamber (temperature range 20–700 °C) with quartz x-ray windows. To avoid contaminations, the materials in contact with the hot, oxidizing gas are chosen to be resistant to this abrasive environment. A schematic side view of the chamber is given in Fig. 2. Earlier experiments using a tubular flow reactor²⁰ showed that by using oxygen and water, etch pits with sufficiently large terraces can be created on $\{111\}$ surfaces. Further, our preliminary surface x-ray experiments on cleaved diamond $\{111\}$ had shown that this face is a good starting point. The method of etching is similar to the gas phase etching experiments in oxygen/water vapor described in Ref. 20, except that here lower etching temperatures of 600–685 °C and shorter etching times of 15–30 min are used. These conditions were chosen in order to avoid a too strong attack of the diamond face causing roughening of the surface, and consequently too strong a reduction in the intensity of the diffracted x rays. Because of these mild conditions, AFM observations on the surfaces before and after etching do not show significant changes in surface morphology.

The diamonds are carefully cleaned by boiling in a mixture of concentrated sulfuric acid and sodium nitrate, heating in aqua regia, and finally by ultrasonic cleaning in demineralized water and in ethanol. After cleaning the diamond substrates are placed in the reaction chamber. Before etching, the setup is sealed off from ambient air and is thoroughly flushed with argon. Then the crystals are heated to the desired etching temperature under an argon flow. The temperature is measured by a thermocouple, which was calibrated to the temperature inside the chamber. To reduce the loss of heat, the quartz cap is covered with aluminum foil. A flow of 10% high-purity oxygen (99.999%) in argon (99.9999%) is

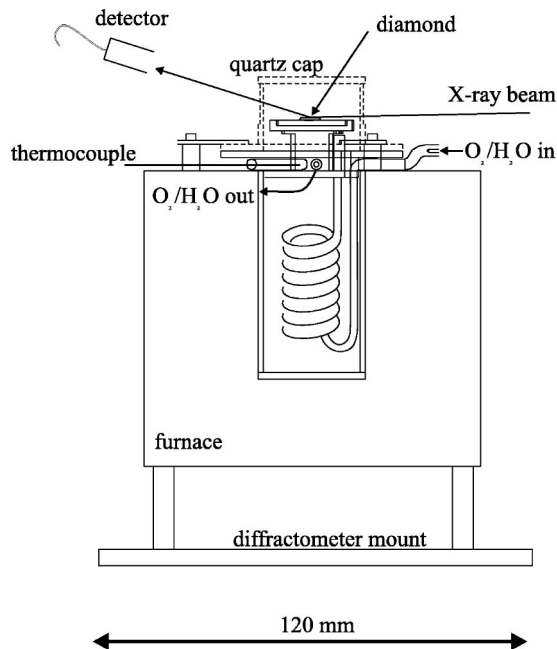


FIG. 2. Side view of the etching chamber. The chamber is cylindrical in shape. The gas that is let in is heated in a coil before the diamond is exposed to it. The quartz cap absorbs a large fraction of the x-ray beam and is therefore removed during the data acquisition.

passed through two flasks containing demineralized, out-gassed water at room temperature (water-vapor pressure ~ 26 mbar). This gas mixture is passed through the reactor during the desired etching period. On completion of the run, the heating is turned off, the aluminum foil is removed and the set-up is allowed to cool down under the same gas mixture. We expect that this procedure leaves the chemical surface structure intact.

B. X-ray measurements

Since carbon is a weak scatterer of x rays, sufficient count rates can only be obtained using a very intense incoming beam.¹⁸ Therefore the high brilliance of a third-generation synchrotron radiation source is needed. We performed our experiments at the surface diffraction undulator beamline ID3 of the European Synchrotron Radiation Facility (Grenoble). A wavelength of 1.07 Å (11.6 keV) was selected using a double-crystal Si(111) monochromator. This relatively low energy (penetration depth) is needed to avoid a too high background signal. On a weak scatterer like diamond, this is a necessary condition to obtain a reasonable signal-to-background ratio. However, this low energy also implies that the penetration of x rays through the quartz window is low. Although we tried to reduce the thickness of the quartz window as much as possible, it absorbed too much signal to perform *in situ* measurements. Therefore, after etching and cooling down to room temperature, the cap of the quartz chamber is removed and the sample is measured in air (relative humidity $\sim 40\%$). The structure did not change over the time scale of days of the experiment, showing that no detectable contamination occurs during the in-air experiments.

We measure intensities along integer-order diffraction rods, the so-called crystal truncation rods (CTR's). These CTR's originate from the abrupt truncation of the crystal lattice at the surface and are diffuse tails to the bulk Bragg peaks. Their intensity is given by the interference between bulk and surface atomic structure. Away from the bulk Bragg points, the surface contribution becomes significant.

In order to denote the diffraction data, we use a surface unit cell for $\{111\}$ diamond. The diamond crystal has an ABC bilayer stacking along the $\langle 111 \rangle$ directions. The primitive surface lattice vectors, expressed in conventional cubic lattice vectors, are $\mathbf{a}_1 = \frac{1}{2}[10\bar{1}]_{\text{cubic}}$, $\mathbf{a}_2 = \frac{1}{2}[\bar{1}10]_{\text{cubic}}$, and $\mathbf{a}_3 = [111]_{\text{cubic}}$. The cubic coordinates are in units of the lattice constant of bulk diamond, 3.567 Å. The corresponding reciprocal lattice vectors $\{\mathbf{b}_j\}$ are given by $\mathbf{a}_i \cdot \mathbf{b}_j = 2\pi\delta_{ij}$. The momentum transfer \mathbf{Q} , which is the difference between the outgoing and the incoming wave vector, is denoted by diffraction indices (hkl) in reciprocal space: $\mathbf{Q} = h\mathbf{b}_1 + k\mathbf{b}_2 + l\mathbf{b}_3$. For crystal truncation rods, which are labeled by (hk) , the indices h and k refer to the in-plane component of the momentum transfer and have integer values, whereas l is unconstrained and refers to its perpendicular component.

The integrated intensity at each point l is determined by rotating the crystal about the surface normal and measuring the number of diffracted photons. The measured intensities are converted to structure factors by applying a standard procedure.²² We find that variation in the etching time and temperature do not result in significant changes in the measured structure factors. In addition, both diamond crystals give similar results, although the data set from the natural diamond was better, as was expected from the AFM measurements. Therefore the data measured for different crystals and etching time and temperatures are merged into one data set. The full data set contains the (10) CTR and specular data ($h=k=0$) (see Fig. 3). The negative part of the (10) rod is obtained by inverting the structure factor distribution along the positive $(\bar{1}0)$ rod through the origin of reciprocal space (Friedel's rule). In total, 224 structure factors were measured, of which 91 were non-equivalent. The average agreement factor of the equivalent reflections and the different preparations is 15%.

III. RESULTS

The analysis of the data is based on fitting the experimental data to structure models by using the ROD program.²³ Diamond is a difficult crystal for x-ray diffraction, and therefore our data set is less precise than for other systems. For this reason it is important to restrict the number of fitting parameters and to use information from other techniques as well. In order to constrain the number of fitting parameters, the Debye-Waller factors for oxygen and carbon are assumed to be isotropic and are fixed at literature values [0.14 for C (Ref. 24), 0.7 for O (Ref. 25)]. Because hydrogen is a very weak x-ray scatterer and has a large vibrational amplitude,²⁶ the hydrogen atoms will only have a small effect on the structure factor. Therefore, throughout the fitting procedures, the relaxation of the hydrogen atoms is coupled to that of the corresponding oxygen atoms.

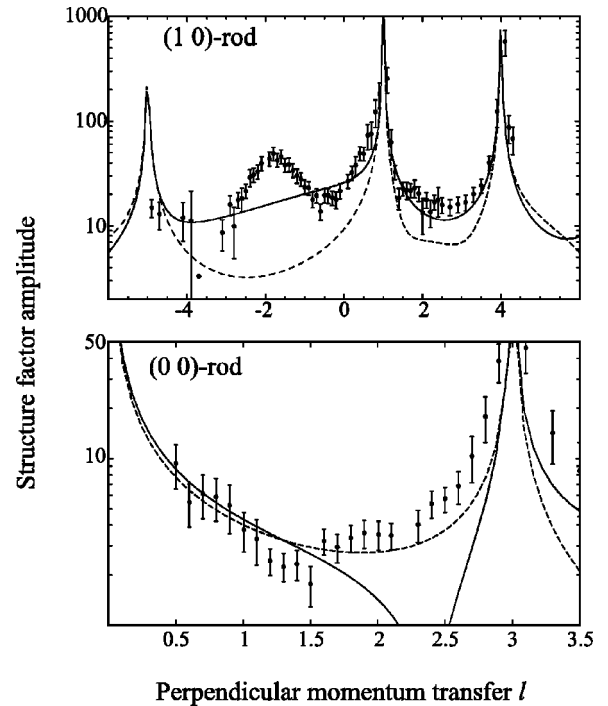


FIG. 3. Structure factor amplitudes along the (10) and (00) CTR as a function of the diffraction index l . The dashed curves represent a calculation for an ideal hydrogen-terminated surface, the solid curves represent a $-\text{OH}$ terminated surface.

There are a number of simple surface structures that one might expect to occur during etching. One possibility is that the surface is hydrogen terminated, with a structure similar to that found by Huisman *et al.*¹⁸ for a polished surface. Model calculations for an ideal, single-cleaved $\{111\}$ diamond surface terminated by hydrogen result in a very high χ^2 value of 12.2 (see Fig. 3), effectively ruling out this possibility. From earlier experiments,²⁰ we expect that species containing monovalent oxygen terminate the etched surface.¹⁴ If we terminate the surface by $-\text{OH}$ groups, however, the calculated model still deviates strongly from the measured data ($\chi^2 = 8.3$), as shown in Fig. 3. Here we have located the oxygen on top of the surface carbon at a distance of 1.43 Å, the value for a single bond between sp^3 bonded carbon and oxygen.²⁷ For these two models, the only free fitting parameter is the overall scale factor. However, it is well known that a diamond surface containing oxygen functionalities is hydrophilic:²⁸ water molecules can form hydrogen bonds with the surface oxygen. Indeed, our specimens etched by oxygen or oxygen and water vapor²⁰ show considerable wetting, as was verified by placing a droplet of water on the surface. This is in contrast to a hydrogen-terminated diamond surface, which is hydrophobic and shows poor wetting. One might thus expect adsorbed water on the etched diamond surfaces. In our model, we therefore add an ordered water layer on top of the diamond surface. The position of the water molecules is set according to energy minimization calculations using the modeling program²⁹ CERIUSt² and is close to the H_3 site [see Fig. 5(b)]. The oxygen atom, and coupled to that the hydrogens of the water molecule, are allowed to relax along the z direction, making the number of

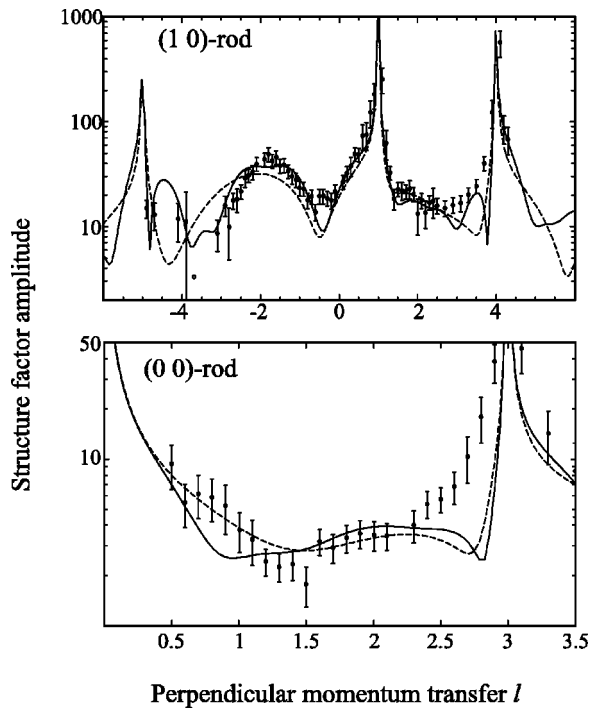


FIG. 4. Structure factor amplitudes along the (1 0) and (0 0) CTR as a function of the diffraction index l . The dashed curves represent a calculation for an ideal —OH terminated surface with one water layer on top, the solid curves represent the best-fit model with one ordered water layer, including relaxations (see text).

free fitting parameters equal to two. The best-fit distance between the oxygen of the —OH group and that of the water molecule is 2.24 \AA . This model gives a much better fit, as shown by the dashed curve of Fig. 4, and has a χ^2 of 4.6. In particular the prominent maximum around $l = -2$ in the (10) rod is fitted much better than in the previous models.

In a further refinement, the surface oxygen and the top three carbon layers are allowed to relax along the z direction. This brings the numbers of free fitting parameters to six. This procedure further reduces χ^2 to 2.5. In order to estimate the oxygen coverage, we allow a fraction γ of the oxygen atoms of the —OH group to be replaced by —H and we release the fraction of the water layer. The best fit, both for the —OH group and the water molecules, is for $\gamma = 1$. This indicates a full monolayer coverage of both —OH and water. To restrict the number of free fitting parameters in our best-fit model, both fractions are subsequently fixed at $\gamma = 1$. This best-fit model is shown by the solid curve in Fig. 4. A side and a top view of this model, a OH -terminated diamond $\{111\}$ surface with an ordered water layer, are shown in Fig. 5. Addition of a second layer of water molecules, at a position above the T_4 site of the substrate as calculated by using CERIUS², does not improve the fit, whereas two extra fitting parameters are needed (the coverage of this water layer and the distance between the water layers).

The optimized atomic distances are given in Table I. Table II shows the coordinates of the surface unit cell based on the best-fit model. It should be noted that, although hydrogen is a very weak scatterer, the models show a better fit if hydrogen is included in the calculations. In a system containing

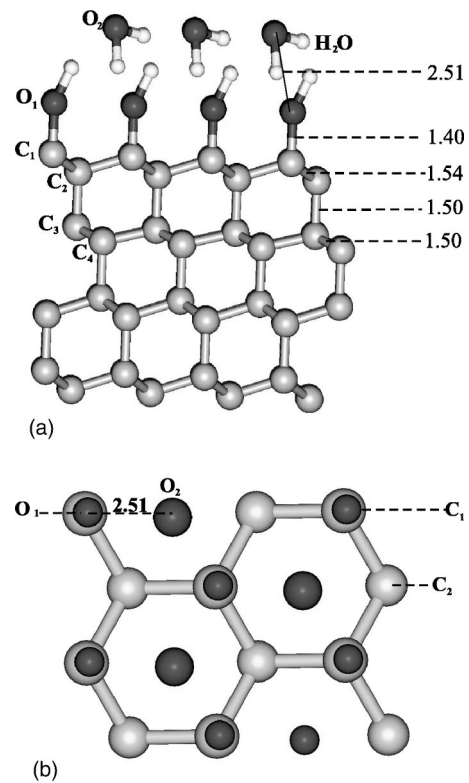


FIG. 5. (a) Side view and (b) top view of the optimized best-fit model of an OH -terminated diamond $\{111\}$ surface with an ordered water layer. The gray spheres represent the carbon atoms, the black spheres the oxygen atoms, and the white spheres the hydrogen atoms (not shown in the top view).

only weak scatterers (carbon, oxygen, hydrogen), the scattering of hydrogen cannot be ignored.

It is clear from Fig. 4 that our best model does not fit the data at all l values. As stated above, given the difficulty of a diamond x-ray diffraction experiment, it is not meaningful to add other fitting parameters. Our aim is to emphasize the most important structural features. We have also tried several other C-O containing terminations involving more complicated bonding topologies or chemical species but none of

TABLE I. Comparison between various structural models and the corresponding best fit parameters. The fixed parameters are indicated with an asterisk.

Parameter	Ideal	—OH terminated	—OH terminated, adsorbed water layer	—OH terminated, adsorbed water layer, relaxations
$d_{\text{O}_2\text{-O}_1}$ (\AA)			2.24 ± 0.05	2.51 ± 0.05
$d_{\text{C}_1\text{-O}_1}$ (\AA)		1.43^*		1.40 ± 0.02
$d_{\text{C}_1\text{-C}_2}$ (\AA)	1.54^*			1.54 ± 0.02
$d_{\text{C}_2\text{-C}_5}$ (\AA)	1.54^*			1.50 ± 0.02
$d_{\text{C}_3\text{-C}_4}$ (\AA)	1.54^*			1.50 ± 0.02
γ_{O_1}				1^*
$\gamma_{\text{H}_2\text{O}}$				1^*
χ^2	12.2	8.3	4.6	2.5

TABLE II. Fractional coordinates of the surface unit cell based on the best fit model of a OH-terminated diamond {111} surface with an ordered water layer.

Element	x	y	z
O ₂	0.74	0.38	0.95±0.03
H ₂	0.78	0.19	0.78
H ₂	0.09	0.76	0.92
O ₁	0.00	0.00	0.61±0.02
H ₁	0.20	0.10	0.77
C ₁	0.00	0.00	0.38±0.02
C ₂	0.33	0.67	0.30±0.02
C ₃	0.33	0.67	0.06±0.02
C ₄	0.67	0.33	0

these yielded a satisfactory fit to the data, as will be discussed in Sec. IV.

IV. DISCUSSION

The data for the etched diamond {111} surface differ completely from the X-ray data measured on oil-polished and solvent-degreased diamond {111} in UHV by Huisman *et al.*¹⁸ From their x-ray data they deduced that their experimental conditions resulted in an average oxygen coverage of about 15% and no water layer. Because of the completely different experimental conditions, such a large difference between their and our data is expected. In our case, oxygen is supplied during the experiment. Many groups found that oxygen chemisorbs easily on diamond. A full monolayer coverage on diamond {001} was found after leaking activated oxygen in UHV below 80 °C.¹⁵ Klauser *et al.*¹⁷ found 0.5 monolayer on {111} diamond after leaking activated oxygen in UHV at room temperature. Another large difference with Huisman *et al.*¹⁸ is that we prepared and measured the surface at atmospheric pressure, therefore the supply of oxygen atoms is orders of magnitude higher compared to the UHV experiments. Many groups found a full oxygen monolayer on diamond powder after oxidation at atmospheric pressure and elevated temperature.^{28,30,31} Our best-fit model also indicates a full monolayer oxygen coverage.

Because an oxygen-terminated diamond surface is hydrophilic,²⁸ one can expect the appearance of a thin water layer. In our model, a monolayer of water is placed on top of the surface. Since these water layers contribute to the measured rods, they must be ordered, both in the lateral and the perpendicular directions. In our best-fit model, the water layer has a coverage of 1. It is possible that additional, disordered water layers are present, which we cannot measure by our technique. The water absorbing properties of diamond surfaces in air are confirmed by AFM measurements.^{32,33} In our best-fit model, the distance between the oxygen of the —OH groups and the oxygen of the water molecules is 2.51 Å. This value is close to the value found for the distance between the oxygen atoms of -P-OH and H₂O for KDP(KH₂PO₄) in an aqueous growth solution, which is 2.52 Å (Ref. 34) and the value found from the energy minimization calculations by CERIU,² which is 2.47 Å.

The appearance of the water layer also helps us to exclude the presence of —CH₃ instead of —OH. If we use the model with one adsorbed water layer and replace the —OH by a methyl group (where the methyl group is placed at a distance of 1.54 Å, the C-C distance in bulk diamond), the fit is not much worse than the fit with —OH ($\chi^2=4.6$ for the —OH model and 5.2 for the —CH₃ model). However, this termination would lead to a hydrophobic diamond surface, and therefore no water layer would appear.

The contractions we find when the structure is allowed to relax in the z direction are similar to those found by Huisman *et al.*¹⁸ on a diamond {111}-(1×1) surface. The contraction of the bilayers corresponds to the results from *ab initio* calculations³⁵ on hydrogen-terminated diamond, although other calculations resulted in essentially no relaxations (molecular dynamics calculations),³⁶ (tight-binding total energy calculations),³⁷ (*ab initio* calculations³⁸). Energy minimization calculations of a full monolayer oxygen on-top of a single-cleaved diamond {111} surface give a C-O distance of 1.34 Å.¹² No H atoms are included in these calculations. The average value for a single bond between sp^3 -bonded carbon and oxygen of an —OH group is 1.43 Å.²⁷ The C-O distance we found in the optimized model is in between those two values, 1.40 Å.

In a previous paper,²⁰ we proposed a surface structure for {111} diamond etched in oxygen/water environment. This model is based on a comparison between the morphology and etch rates of diamond {111} etched by various oxidative methods. Etching proceeds layerwise via monoatomic steps, indicating that the surface is stabilized by the etching compounds. This is in contrast to dry oxygen etching, where the divalent oxygen causes chemical roughening. The structure we proposed for oxygen/water etching starts from a diamond {111} surface terminated by single dangling bonds that are stabilized by monovalent compounds, like —OH and —H. Our X-ray data provide strong evidence that the monovalent surface compound is —OH and not —H.

Many groups propose the presence of C-O-C (ether) and C=O (ketone) groups.^{12,28,30,31} To test the presence of ether groups, we took the calculated models of Zheng and Smith¹² as a starting point. Models containing oxygen at each alternating bridge site on (1) an undistorted {111} surface terminated by one dangling bond and on (2) a (2×1) reconstructed {111} surface terminated by three dangling bonds are tested. These models give a fit comparable to that of our —OH terminated model, but in contrast to this model, the fits get worse upon the addition of a water layer. Second, a full monolayer of oxygen on (1) an undistorted surface terminated by three dangling bonds and (2) a (2×1) reconstructed surface terminated by three dangling bonds is examined. These two models both result in a poor fit to the data. The presence of C=O (ketone) in our model is also not likely. The distance we found between C and O is 1.40 Å, which is much closer to the value for a single bond between sp^3 -bonded carbon and oxygen [1.43 Å (Ref. 27)] than to that for a double bond between C and O [1.23 Å (Ref. 27)]. Further, the tetravalent carbon in C=O can only be present on the single cleaved surface as HC=O. Energy minimiza-

tion using CERIUSt² showed that this extra H atom sterically does not fit on the closely packed diamond {111} surface.

From their calculations, Zheng and Smith¹² deduced that a C-O-O-C (peroxide) was the most stable full-monolayer coverage on {111} diamond terminated by one dangling bond. This compound is not likely to exist in our system, because a CO-OC bond is weak compared to a CO-H bond [38 versus 105 kcal/mol (Ref. 39)]. In the presence of hydrogen, it will rapidly convert into —OH. Finally, lactone [-C(=O)-O-C] and anhydride [-C(=O)-O-O(=O)-] structures are proposed by Ando *et al.*³¹ Again, energy minimization showed that these large compounds are not likely from a sterical point of view.

In this experiment we determine the atomic structure of the {111} diamond face after wet oxygen etching. The surface is studied in air at room temperature, and we find a well-ordered water layer on the top of the —OH terminated surface. To fully understand the etching mechanism, the setup needs to be improved so that the surface can be studied during etching. It would be interesting to study what happens to the water layers at the high temperatures present during etching.

V. CONCLUSIONS

We have used the technique of surface x-ray diffraction to study the structure of {111} diamond after etching in oxygen and water vapor. The model that fits the data best is a single cleaved diamond {111} surface model with the dangling bond saturated by a full monolayer of —OH. To explain the mea-

surements it is necessary to add an ordered water layer on top of the —OH terminated surface. Small relaxations are found in the first four layer spacings. The contraction between the first two bilayers agrees with earlier measurements¹⁸ and calculations.³⁵ The best-fit distance between the oxygen of the —OH groups and the oxygen of the water molecules corresponds to the value found from the energy minimisation calculations by CERIUSt² and the value found for the distance between the oxygen atoms of -P-OH and H₂O for KDP in an aqueous growth solution. The results of this study gives experimental evidence to support the atomic structure of the terrace atoms, as proposed in our previous paper²⁰ and explains the relative stability of diamond {111} under these etching conditions.

ACKNOWLEDGMENTS

The authors wish to thank P. van Dijk, A. Engels, J. Haerckens, H. Verscharen, and P. Walraven for their technical support in constructing and building the etching setup. We also are grateful to J. van de Streek for performing the energy minimizations and for useful discussions, to Dr. O. Robach and Dr. M. Plomp for their help during the surface x-ray diffraction experiments and to Dr. A. Klunder who helped us to understand the organic chemistry behind this system. This work was performed as part of the research program of the Council for Chemical Sciences (CW) and the Foundation for Fundamental Research on Matter (FOM) with financial support from the Dutch Organization for Scientific Research (NWO).

*Author to whom correspondence should be addressed. Electronic address: vlieg@sci.kun.nl

¹S. J. Harris and A. M. Weiner, *Appl. Phys. Lett.* **55**, 2179 (1989).

²T. Kawato and K.-I. Kondo, *Jpn. J. Appl. Phys., Part 1* **26**, 1429 (1987).

³L. S. G. Plano, in *Diamond: Electronic Properties and Applications*, edited by L. S. Pan and D. R. Kania (Kluwer, Dordrecht, 1995), p. 31.

⁴Y. Liou, R. Weimer, D. Knight, and R. Messier, *Appl. Phys. Lett.* **56**, 437 (1990).

⁵S. J. Harris and A. M. Weiner, *Appl. Phys. Lett.* **55**, 2179 (1989).

⁶M. Ikeda, E. Mizuno, M. Hori, T. Goto, K. Yamada, M. Hiramatsu, and M. Nawata, *Jpn. J. Appl. Phys., Part 1* **35**, 4826 (1996).

⁷P. Badziag and W. S. Verwoerd, *Surf. Sci.* **183**, 469 (1987).

⁸M. Frenklach, D. Huang, R. E. Thomas, R. A. Rudder, and R. J. Markunas, *Appl. Phys. Lett.* **63**, 3090 (1993).

⁹J. Robertson and M. J. Rutten, *Diamond Relat. Mater.* **7**, 620 (1998).

¹⁰S. Skokov, B. Weiner, and M. Frenklach, *Phys. Rev. B* **49**, 11 374 (1994).

¹¹J. L. Whitten, P. Cremaschi, R. E. Thomas, R. A. Rudder, and R. J. Markunas, *Appl. Surf. Sci.* **75**, 45 (1994).

¹²X. M. Zheng and P. W. Smith, *Surf. Sci.* **262**, 219 (1992).

¹³S. Skokov, B. Weiner, and M. Frenklach, *Phys. Rev. B* **55**, 1895 (1997).

¹⁴F. K. de Theije, N. J. van der Laag, M. Plomp, and W. J. P. van Enckevort, *Philos. Mag. A* **80**, 725 (2000).

¹⁵P. E. Pehrsson and T. W. Mercer, *Surf. Sci.* **460**, 49 (2000).

¹⁶P. E. Pehrsson and T. W. Mercer, *Surf. Sci.* **460**, 74 (2000).

¹⁷R. Klauser, J. Chen, T. Chuang, L. Chen, M. Shih, and J. Lin, *Surf. Sci.* **356**, L410 (1996).

¹⁸W. J. Huisman, J. F. Peters, S. A. de Vries, E. Vlieg, W. S. Yang, T. E. Derry, and J. F. van der Veen, *Surf. Sci.* **387**, 342 (1997).

¹⁹P. Steadman, K. Peters, H. Isern, J. Alvarez, and S. Ferrer, *Phys. Rev. B* **62**, R2295 (2000).

²⁰F. K. de Theije, E. van Veenendaal, W. J. P. van Enckevort, and E. Vlieg, *Surf. Sci.* (to be published).

²¹F. K. de Theije, O. Roy, N. van der Laag, and W. J. P. van Enckevort, *Diamond Relat. Mater.* **9**, 929 (2000).

²²E. Vlieg, *J. Appl. Crystallogr.* **30**, 532 (1997).

²³E. Vlieg, *J. Appl. Crystallogr.* **33**, 401 (2000).

²⁴H. X. Gao and L.-M. Peng, *Acta Crystallogr., Sect. A: Cryst. Phys., Diffr., Theor. Gen. Crystallogr.* **55**, 926 (1999).

²⁵C. Y. Liao, S. H. Chen, and F. Sette, *Phys. Rev. E* **61**, 1518 (2000).

²⁶B. Sandfort, A. Mazur, and J. Pollmann, *Phys. Rev. B* **51**, 7168 (1995).

²⁷*CRC Handbook of Chemistry and Physics*, 1st student ed., edited by R. C. Weast (CRC Press, Boca Raton, 1990) p. F107.

²⁸R. Sappok and H. Boehm, *Carbon* **6**, 573 (1968).

²⁹CERIUSt² (Molecular Simulations, San Diego, 1997).

- ³⁰S. Matsumoto, H. Kanda, Y. Sato, and N. Setaka, *Carbon* **15**, 299 (1977).
- ³¹T. Ando, K. Yamamoto, M. Ishii, M. Kamo, and Y. Sato, *J. Chem. Soc., Faraday Trans.* **89**, 3635 (1993).
- ³²H. G. Maguire, M. Kamo, H. P. Lang, and H.-J. Guntherodt, *Appl. Surf. Sci.* **60/61**, 301 (1992).
- ³³H. G. Maguire, M. Kamo, H. P. Lang, and H.-J. Guntherodt, *Appl. Surf. Sci.* **75**, 144 (1994).
- ³⁴M. F. Reedijk, J. Arsic, F. F. A. Hollander, S. A. de Vries, and E. Vlieg (unpublished).
- ³⁵D. R. Alfonso, D. A. Drabolt, and S. E. Ulloa, *Phys. Rev. B* **51**, 14 669 (1995).
- ³⁶Th. Frauenheim, U. Stephan, P. Blaudeck, D. Porezag, H.-G. Busmann, W. Zimmermann-Edling, and S. Lauer, *Phys. Rev. B* **48**, 18 189 (1993).
- ³⁷B. N. Davidson and W. E. Pickett, *Phys. Rev. B* **49**, 14 770 (1994).
- ³⁸G. Kern, J. Hafner, and G. Kresse, *Surf. Sci.* **366**, 445 (1996).
- ³⁹CRC Handbook of Chemistry and Physics, 1st student ed., edited by R. C. Weast (CRC Press, Boca Raton, 1990), pp. F125–126.